Polym. Bull. (2012) 68:299–308
DOI 10.1007/s00289-011-0532-x

ORIGINAL PAPER

Synthesis of well-dispersed polyimide/TiO_2 nanohybrid films using a pyridine-containing aromatic diamine

Hojjat Seyedjamali · Azadeh Pirisedigh

Received: 7 January 2011 / Revised: 15 May 2011 / Accepted: 30 May 2011 /
Published online: 11 June 2011

Abstract The sol–gel fabrication of new well-dispersed polyimide (PI)/TiO_2 nanohybrid films is reported. The PI matrixes are synthesized via the polycondensation of pyromellitic dianhydride and a diamine monomer containing several constructive functional groups which introduced some interesting features to the final nanocomposite (NC) materials. The TiO_2–heteroatom interactions associated with the flexible characteristic of polymer backbone (which facilitates the stated interactions) have been led to the fabrication of well-dispersed nanoparticles with less than 100 nm in sizes, as confirmed by means of transmission electron microscopy. Thermal analysis techniques (TGA and DSC) have shown the superior thermal stability of fabricated NCs. The UV–Vis spectroscopy has illustrated a growing trend in the absorption efficiency along with the increase in TiO_2 contents. The created TiO_2 nanoparticles showed amorphous structures according to the X-ray diffraction patterns.

Keywords Nanocomposite · Sol–gel · Polyimide · TiO_2

Introduction

In the last decade, the fabrication and properties of organic/inorganic nanocomposites (NCs) have attracted many attentions [1–3]. These innovative materials have been employed for various contemporary applications such as biomaterials [4], waveguides [5], nonlinear optical devices [6], electrolytes [7], fuel cells [8], gas separation membranes [9] and proton conductive membranes [10]. Between the wide varieties of existing organic/inorganic NCs, polyimide (PI)/TiO_2 nanohybrid

H. Seyedjamali (✉) · A. Pirisedigh
Department of Chemistry, Islamic Azad University, Kazerun Branch, Kazerun, Iran
e-mail: seyedjamali@yahoo.com; hojjat.seyedjamali@kau.ac.ir

materials possess an exceptional situation due to the interesting properties of each component [11–14].

The PIs are known as imperative composite matrixes, because of the excellent thermo-chemical resistances, outstanding mechanical properties and low dielectric constant [15–18] and TiO_2 nanoparticles have the wide range of academic and industrial consumptions due to the photo-catalytic activity, high refracting index and of course low costs [19, 20].

The dispersion of nanoparticles in the composite grounds affects extremely the nanodimensional properties of final NCs. The intensive improvements in NCs properties will be observable when nanoparticles are well dispersed in NC grounds [21]. Several approaches have been already introduced to improve the distribution of inorganic nanoparticles in the polymer matrixes including the use of various dispersants which couple the organic/inorganic phases via either chemical bonds or physical interactions [22, 23]. Phosphate, silicate, thiol, methacrylic acid and polymeric linkers are some of the usual coupling agents which regulate the dispersion of nanohybrid materials covalently [23, 24].

A further important technique is the in situ sol–gel synthesis of nanoparticles within composite matrix. This linker-free manner for the production of nanohybrid materials is preferred due to the more simplicity and dispensable preconditions as well as the easy controlling of the concentrations of organic and inorganic components in the solution [9, 25, 26]. Fortunately, the synthesis of PIs via the polycondensation of diamines (DA) and dianhydrides enjoys a high adjustment with the sol–gel technique. Of course, in the sol–gel procedure, the possible agglomeration and aggregation of nanoparticles—as a result of the fast gelations—may diminish the dispersion of nanoparticles in the polymer grounds. The use of a chelating agent is an useful approach to manage the rate of gelation step [25]. Another effective strategy is the application of a polymeric matrix containing suitable functional groups to coordinate to inorganic nanoparticles. Recently, we have reported the fabrication of a series of well-dispersed PI/TiO_2 NCs which were well dispersed by means of aforementioned issue [27]. In this study, we wish to report the fabrication of well-dispersed TiO_2 nanoparticles within flexible PI matrix through a sol–gel procedure. Typically, the increase in polymers flexibility achieves via the introduction of asymmetric, flexible and/or bulky moieties in the main chain as well as pendant groups [15, 27–30].

Experimental

Materials

All chemicals were purchased from Fluka Chemical Co. (Buchs, Switzerland), Aldrich Chemical Co. (Milwaukee, WI), Riedel–deHaen AG (Seelze, Germany) and Merck Chemical Co. Pyromellitic dianhydride (PMDA) was recrystallized from acetic anhydride and then dried in a vacuum oven at 120 °C overnight. *N*,*N*-dimethylacetamide (DMAc) was dried over barium oxide, followed by

fractional distillation. Tetraethyl orthotitanate ($Ti(OEt)_4$) and acetylacetone (acac) were employed as received.

Equipments

FT-IR spectra were recorded on 400D IR spectrophotometer (Japan). The spectra were obtained using KBr pellets. The vibrational transition frequencies are reported in wave numbers (cm^{-1}). Band intensities are assigned as weak (w), medium (m), strong (s) and broad (br). Thermal gravimetric analysis (TGA) data were taken on Perkin Elmer in nitrogen atmosphere at a heating rate of 20 °C min^{-1}. Differential scanning calorimetry (DSC) data were recorded on a DSC-PL-1200 instrument at a heating rate of 20 °C min^{-1} in nitrogen atmosphere. The glass transition temperatures (T_g) were read at the middle of the transition in the heat capacity taken from the heating DSC traces. The X-ray diffraction (XRD) patterns were recorded by employing a Philips X'PERT MPD diffractometer (Cu Kα radiation: $\lambda = 0.154056$ nm at 40 kV and 30 mA) over the 2θ range of 20°–80° at a scan rate of 0.05° min^{-1}. Transmission electron microscopy (TEM) images were recorded using a JEOL JEM-2000.

Synthesis of DA

4-Phenyl-2,6-bis[3-(4-aminophenoxy)phenyl]pyridine (DA) was synthesized according to the procedure recently reported by Yi et al. [15].

Synthesis of PI/TiO_2 NCs films

The PMDA was added gradually to a DMAc solution of DA (with the molar ratios of 1:1) under dry conditions at 0 °C. The fresh part of PMDA was added next to the complete dissolution of prior part. After the complete addition of PMDA, the mixture was stirred for 2 h at room temperature to achieve the corresponding solution of poly(amic acid) (PAA). Then required amounts of $Ti(OEt)_4$/acac (with molar ratios of 1:4) was added and the mixture was further stirred for 15 h. The concentrations of TiO_2 were 2, 4, 6, 8 and 10 wt% assuming the absolute conversion of $Ti(OEt)_4$ to TiO_2 particles. Thin films of pure PAA and mixed PAA with various percentages of TiO_2 precursor were prepared through casting onto dust-free glass plates. Produced films were annealed under a dynamic air atmosphere oven at 70, 100, 150, 200 and 250 °C for 1 h each and 300 °C for 12 h. After the complete imidization of PAA, the films were cooled to room temperature and removed from the glass surfaces using a razor blade. Abbreviations as NCT2–NCT10 are corresponded to the NCs with 2–10 wt% TiO_2 contents, respectively.

PAA: IR (KBr): ν = 2350–3750 (br), 1736 (s), 1724 (s), 1606 (s), 1537 (s), 1497 (s), 1402 (s), 1212 (m), 1013 (m), 826 (m), 511(m) cm^{-1}.

Pure polymer matrix: IR (KBr): ν = 3061 (w), 1777 (m), 1733 (s), 1724 (s), 1626 (m), 1592 (s), 1499 (s), 1360 (s), 1010 (w), 869 (m), 425 (m), 597 (w) cm^{-1}.

NCT2: IR (KBr): ν = 3058 (br), 1777 (w), 1734 (s), 1720 (S), 1500 (s), 1377 (s), 1239 (m), 820 (w), 724 (w), 746 (w), 603 (w), 518 (w), 444 (w) cm^{-1}.

NCT4: IR (KBr): ν = 3060 (w), 1774 (w), 1738 (s), 1721 (s), 1498 (s), 1374 (m), 1238 (m), 821 (m), 725 (m), 604 (m), 517 (m), 447 (m) cm^{-1}.

NCT6: IR (KBr): ν = 3059 (w), 1776 (w), 1735 (s), 1721 (s), 1499 (s), 1376 (m), 1241 (m), 1037 (m), 625 (br), 520 (s), 471 (s) cm^{-1}.

NCT8: IR (KBr): ν = 3062 (w), 1770 (w), 1738 (s), 1723 (s), 1501 (s), 1373 (m), 1242 (m), 1035 (m), 622 (s), 521 (s), 473 (s) cm^{-1}.

NCT10: IR (KBr): ν = 3065 (w), 1772 (w), 1740 (s), 1724 (s), 1498 (s), 1379 (m), 1238 (m), 1038 (m), 626 (s), 518 (s), 469 (s) cm^{-1}.

Results and discussion

Preparation of NCs

The reaction of DA and PMDA was carried out at room temperature to suspend the reaction at the PAA formation stage (Scheme 1). The resulted PAA was mixed with desired quantities of $Ti(OEt)_4$/acac solutions (1:4). After homogenization and film casting the prepared films were annealed gradually. The water generated during the thermal imidization of amic acid moieties hydrolyzed the titanate agent to TiO_2 nanoparticles. The amounts of supplied TiO_2 were measured to be in the range of 2–10 wt% supposing the complete conversion of titanate agent.

The role of acac was to diminish the hydrolysis rate of titanate to manage the rapid gelation and/or phase separation. Since, a controlled gelation will cause the more consistent particles size, distribution and shape. Thin films of the stated crude mixtures were prepared and then annealed gradually up to 300 °C and kept on at this temperature for confident quantitative imidization.

Prepared NC thin films were characterized by means of FT-IR, UV–Vis, TEM, TGA and DSC analyses. Figure 1 consists of the FT-IR spectra of crude PAA, pure polymer matrix and NCT2–NCT10 thin films. A broad absorption peak is obvious at 2350–3750 cm^{-1} in the spectrum of PAA corresponding to the carboxylic acid moieties which is omitted in the spectrum of the other entries confirming the complete imidization of PAA. The broad absorption peaks related to the Ti–O bands appeared in the spectra of NCT2–NCT10 at 400–800 cm^{-1} and became more intensive with the increase in TiO_2 percentages.

Characteristics

The TGA analysis was used to evaluate the thermal properties of fabricated NCs and the results are shown in Fig. 2. Obviously, the char yields of NCs at 800 °C are increased from pure polymer matrix to NCT10 confirming the superior thermal stability due to the more nanosized inorganic contents. However, a tiny shrink in the thermal resistances at lower temperatures is visible which may be discussed by means of the familiar oxidative decomposition of polymer ground catalyzed by metal oxide component [11–14, 16] especially in the case of NCT10 with the highest TiO_2 percentage. In addition, unpaired electrons related to the heteroatoms may induce the oxidative decomposition of polymer matrix [14].

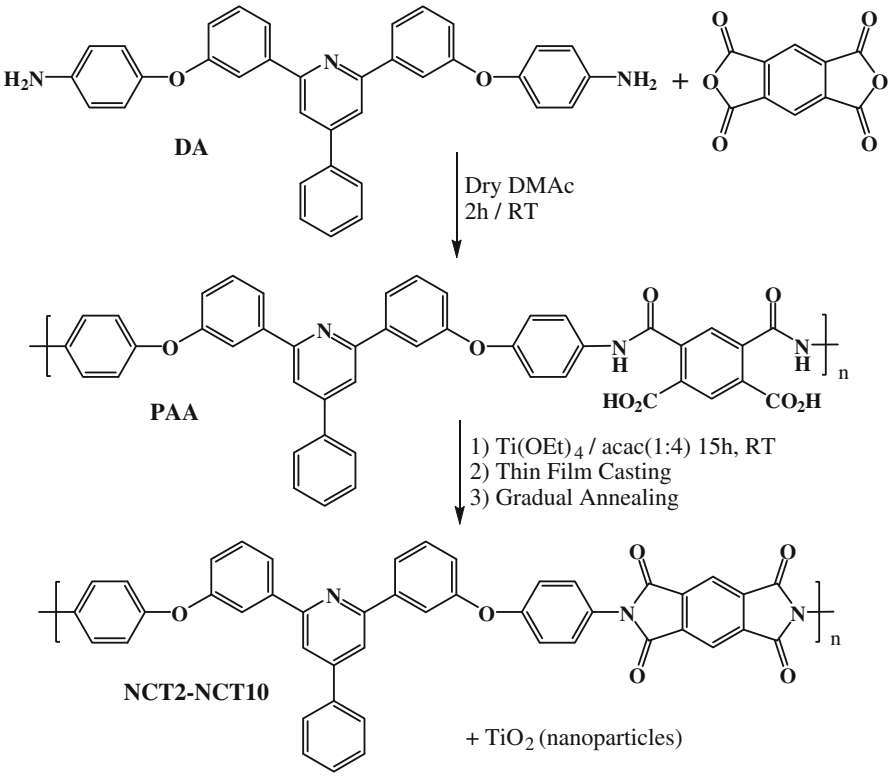

Scheme 1 Synthesis pathway for NCs with various TiO_2 contents

In order to verify the temperature in which the imidization occurs, the TGA thermogram of PAA was recorded as well. A substantial weight loss initiated at 170 °C related to the evaporation of water—produced through the condensation of amic acid moieties to imide functions—reveals the starting point of imidization. This instructive thermogram confirms the complete imidization temperature to be at 300 °C. The DSC analysis was used to determine the T_g values of fabricated NCs as well as pure polymer ground (Table 1). The results shows the enhancements in T_g values as a function of increase in TiO_2 percentage which may well be discussed by the limited segmental motion due to the rather strong organic–inorganic interaction.

Several well-dispersed TiO_2 regions are observable in the TEM photographs of NCs (Fig. 3). The nanoparticles sizes were determined to be in the range of 20–100 nm. Obviously, the lower TiO_2 contents not only have led to the formation of smaller particles sizes but also to obtain the superior dispersion of particles. This observation may be related to the faster gelation step and more nanoparticles aggregation at the higher TiO_2 concentrations. The interactions of nonbonding electrons (existing in either nitrogen or oxygen atoms) and TiO_2 are responsible for well-dispersion of nanoparticles. On the other hand, the use of flexible polymer matrixes has led to the acceptable particle distributions due to the facilitated

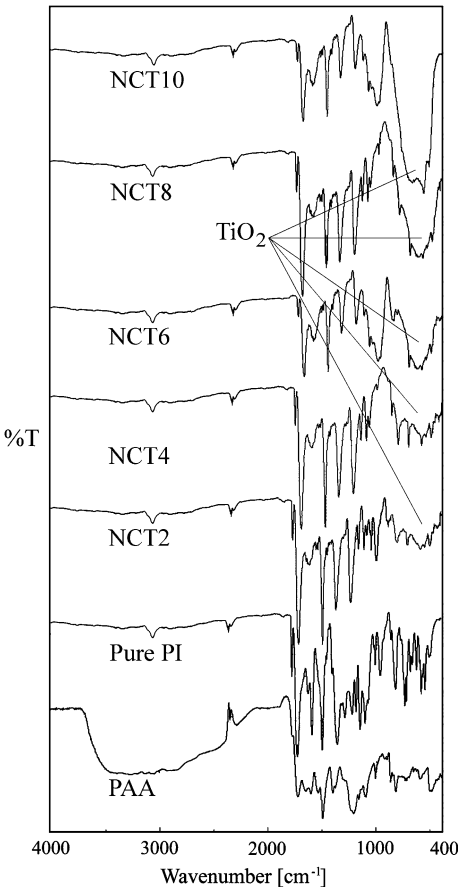

Fig. 1 FT-IR spectra of PAA, pure polymer matrix and NCT2–NCT10

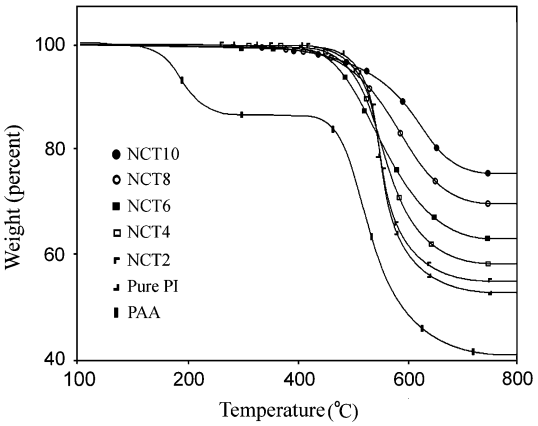

Fig. 2 TGA thermograms of PAA, pure polymer matrix and NCT2–NCT10

organic/inorganic interactions. The comparison of this study with related study confirms that the use of more flexible polymers lead to the improvements in nanoparticles distributions [11, 25].

Table 1 The T_g values measured using DSC analyses

Entry	Sample	T_g (°C)[a]
1	Pure PI	235.4
2	NCT2	239.2
3	NCT4	247.9
4	NCT6	255.3
5	NCT8	264.2
6	NCT10	273.1

[a] Measured at a heating rate of 20 °C/min under N_2 atmosphere

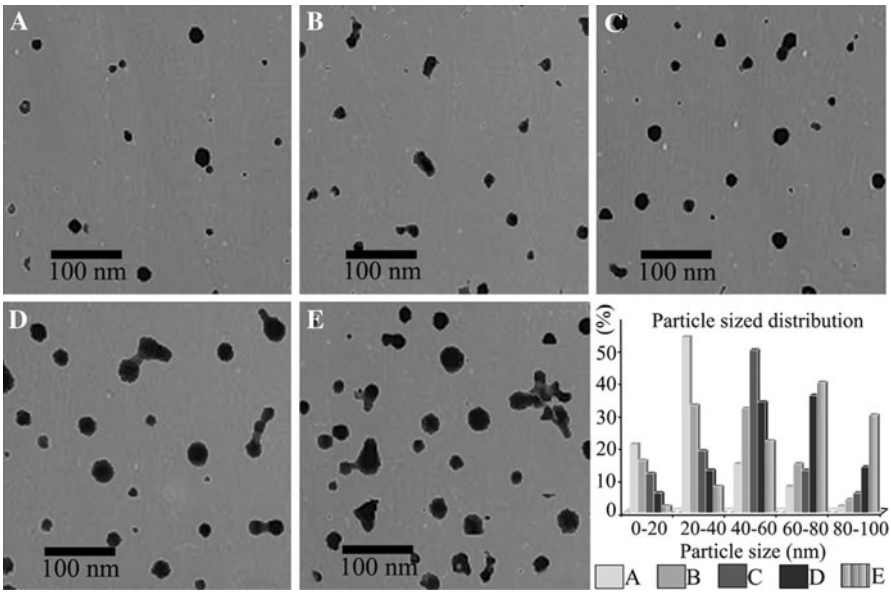

Fig. 3 TEM photographs of NCs with 2% (**a**), 4% (**b**), 6% (**c**), 8% (**d**) and 10% (**e**) of TiO_2 and their size distribution diagrams

The UV–Vis spectra of polymer matrix and NCs with different TiO_2 contents, illustrated in Fig. 4, confirms that the greater TiO_2 percentage has caused the smaller *T%* which may be attributed to the more aggregation of TiO_2 particles and/or the creation of titanium ion–acac complex. However, the complex formation mechanism may be minor following the gelation step [31].

The XRD patterns of the polymer matrix and some representative NCs are shown in Fig. 5. The other NCs showed comparatively the same patterns. Expectedly, the described procedure was led to the formation of amorphous TiO_2 [11]. Moreover, the losing of partial crystallinity of polymer matrix may be concluded from the comparison of XRD spectra which could be described by the creation of scarce TiO_2 cluster size and/or relatively strong polymer–TiO_2 interactions.

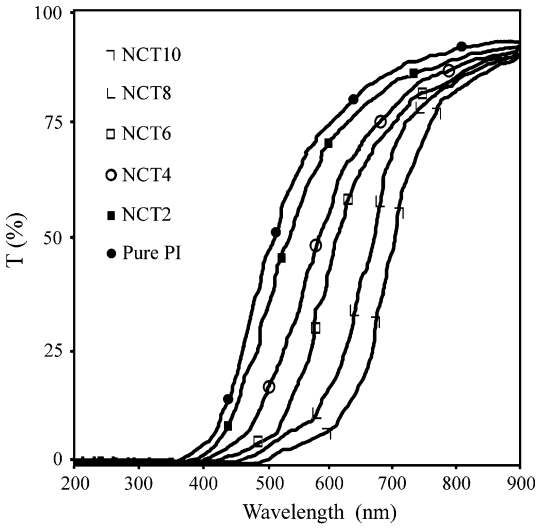

Fig. 4 UV–Vis spectra of pure polymer matrix and NCT2–NCT10

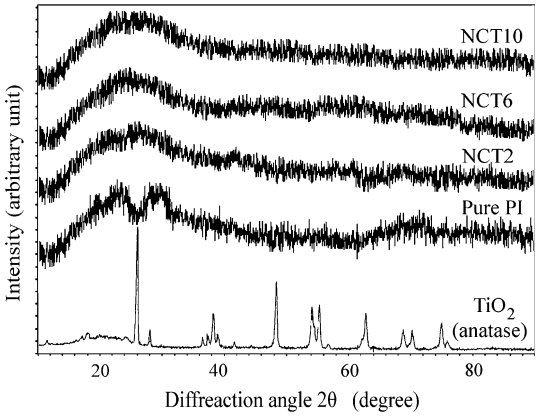

Fig. 5 XRD patterns of pure TiO_2 (anatase), pure polymer matrix and some typical NCs

Conclusions

In this study, a flexible bulky diamine monomer (DA) was used for the synthesis of new brand of functional PI/TiO_2 NCs thin films. Polycondensations of the stated DA with an aromatic dianhydride (PMDA) proceed in two steps under dry conditions in the presence of various concentration of alkoxy titanate agent as TiO_2 precursor. Thin films of crude PAA/titanate mixtures (with 2–10 wt%) were cast and experienced the gradual thermal annealing to produce corresponding NCs through the in situ sol–gel procedure. The TEM imaging of NCs with various TiO_2 percentages confirms the created nanoparticles to be in the size ranges of 20–100 nm and well dispersed. These characteristics may be attributed to the existing of various functional groups in the structure of polymer ground. For instance, the existence of both ether functions and phenyl pendant groups made the

polymer chain flexible enough to interact (via either nitrogen or oxygen lone pairs) with TiO_2 properly. The thermal analysis (TGA and DSC) of NCs confirms their elevated heat resistance. The UV–Vis spectroscopy confirmed the higher blocking efficiency with the increase in TiO_2 contents. The XRD pattern showed the NCs to be amorphous.

Acknowledgments Financial support for this study from Research Affairs Division, Islamic Azad University, Kazerun Branch, Iran, and Iran nanotechnology Initiative Council and National Elite Foundation (NEF) is greatly acknowledged.

References

1. Mahdavian AR, Sarrafi Y, Shabankareh M (2009) Nanocomposite particles with core–shell morphology III: preparation and characterization of nano Al_2O_3–poly(styrene–methyl methacrylate) particles via miniemulsion polymerization. Polym Bull 63:329–340
2. Khan AA, Khan A (2010) Ion-exchange studies on poly-*o*-anisidine Sn(IV) phosphate nano composite and its application as Cd(II) ion-selective membrane electrode. Cent Eur J Chem 8:396–408
3. Lin D-J, Chen C-C, Chang C-L, Su Y-C, Cheng L-P (2002) Observation of nano-particles in silica/poly(HEMA) hybrid by electron microscopy. J Polym Res 9:115–118
4. Shin MK, Spinks GM, Shin SR, Kim SI, Kim SJ (2009) Nanocomposite hydrogel with high toughness for bioactuators. Adv Mater 21:1712–1715
5. Sirbuly DJ, Letant SE, Ratto TV (2008) Hydrogen sensing with subwavelength optical waveguides via porous silsesquioxane–palladium nanocomposites. Adv Mater 20:4724–4727
6. Pandey RK, Sandeep CSS, Philip R, Lakshminarayanan V (2009) Enhanced optical nonlinearity of polyaniline–porphyrin nanocomposite. J Phys Chem C 113:8630–8634
7. Zhang W, Li MKS, Yue P-L, Gao P (2008) Exfoliated Pt-clay/nafion nanocomposite membrane for self-humidifying polymer electrolyte fuel cells. Langmuir 24:2663–2670
8. Liao S-H, Weng C-C, Yen C-Y, Hsiao M-C, Ma C-CM, Tsai M-C, Su A, Yen M-Y, Lin Y-F, Liu P-L (2010) Preparation and properties of functionalized multiwalled carbon nanotubes/polypropylene nanocomposite bipolar plates for polymer electrolyte membrane fuel cells. J Power Sources 195:263–270
9. Cong H, Radosz M, Towler BF, Shen Y (2007) Polymer–inorganic nanocomposite membranes for gas separation. Sep Purif Technol 55:281–291
10. Lakshminarayana G, Nogami M (2009) Synthesis and characterization of proton conducting inorganic-organic hybrid nanocomposite membranes based on mixed PWA-PMA-TEOS-GPTMS-H3PO4-APTES for H_2/O_2 Fuel Cells. J Phys Chem C 113:14540–14550
11. Chiang P-C, Whang W-T (2003) The synthesis and morphology characteristic study of BAO-ODPA polyimide/TiO_2 nano hybrid films. Polymer 44:2249–2254
12. Tsai M-H, Chang C-J, Chen P-J, Ko C-J (2008) Preparation and characteristics of poly(amide–imide)/titania nanocomposite thin films. Thin Solid Films 516:5654–5658
13. Liaw W-C, Chen K-P (2007) Preparation and characterization of poly(imide siloxane) (PIS)/titania (TiO_2) hybrid nanocomposites by sol–gel processes. Eur Polym J 43:2265–2278
14. Liu L, Qinghua L, Jie Y, Xuefeng Q, Wenkai W, Zikang Z, Zongguang W (2002) Photosensitive polyimide (PSPI) materials containing inorganic nano particles (I)PSPI/TiO_2 hybrid materials by sol–gel process. Mater Chem Phys 74:210–213
15. Yan S, Chen W, Yang X, Chen C, Huang M, Xu Z, Yeung KWK, Yi C (2011) Soluble polyimides based on a novel pyridine-containing diamine m,p-PAPP and various aromatic dianhydrides. Polym Bull 66:1191–1206
16. Tsai M-H, Huanga S-L, Chena P-J, Chiang P-C, Chena D-S, Luc H-H, Chiua W-M, Chend J-C, Lua H-T (2008) Characteristics and properties of polyimide/vanadium oxide hybrid membranes. Desalination 233:232–238
17. Tsai M-H, Whang W-T (2001) Low dielectric polyimide/poly(silsesquioxane)-like nanocomposite material. Polymer 42:4197–4207

18. Tsai M-H, Chiang P-C, Whang W-T, Ko C-J, Huang S-L (2006) Synthesis and characteristics of polyimide/siloxane hybrid films for reliability adhesion. Surf Coat Technol 200:3297–3302
19. Owpradit W, Jongsomjit B (2008) A comparative study on synthesis of LLDPE/TiO_2 nanocomposites using different TiO_2 by in situ polymerization with zirconocene/dMMAO catalyst. Mater Chem Phys 112:954–961
20. Severn JR, Chadwick JC, Duchateau R, Friederichs N (2005) Bound but not gagged immobilizing single-site α-olefin polymerization catalysts. Chem Rev 105:4073–4147
21. Tang E, Cheng G, Pang X, Ma X, Xing F (2006) Synthesis of nano-ZnO/poly(methyl methacrylate) composite microsphere through emulsion polymerization and its UV-shielding property. Colloid Polym Sci 284:422–428
22. Zou H, Wu S, Shen J (2008) Polymer/silica nanocomposites: preparation, characterization, properties, and applications. Chem Rev 108:3893–3957
23. Khaled SM, Sui R, Charpentier PA, Rizkalla AS (2007) Synthesis of TiO_2–PMMA nanocomposite: using methacrylic acid as a coupling agent. Langmuir 23:3988–3995
24. Sanchez C, Soler-Illia GJDAA, Ribot F, Lalot T, Mayer CR, Cabui V (2001) Designed hybrid organic–inorganic nanocomposites from functional nanobuilding blocks. Chem Mater 13:3061–3083
25. Hu Q, Marand E (1999) In situ formation of nanosized TiO_2 domains within poly(amide–imide) by a sol–gel process. Polymer 40:4833–4843
26. Czarnobaj K (2011) Sol–gel-processed silica/polydimethylsiloxane/calcium xerogels as polymeric matrices for metronidazole delivery system. Polym Bull 66:223–237
27. Seyedjamali H, Pirisedigh A (2010) In situ sol–gel fabrication of new poly(amide–ether–imide)/titania (TiO_2) nanocomposite thin films containing L-leucine moieties. Colloid Polym Sci 289:15–20
28. Kim YJ, Chung IS, In I, Kim SY (2005) Soluble rigid rod-like polyimides and polyamides containing curable pendent groups. Polymer 46:3992–4004
29. Zulfiqar S, Lieberwirth I, Sarwar MI (2008) Soluble aramid containing ether linkages: synthesis, static and dynamic light scattering studies. Chem Phys 344:202–208
30. Behniafar H, Boland P (2010) Heat stable and organosoluble polyimides containing laterally-attached phenoxy phenylene groups. J Polym Res 17:511–518
31. Que W, Zhou Y, Lam YL, Chan YC, Kam CH (2000) Optical and microstructural properties of sol–gel derived titania/organically modified silane thin films. Thin Solid Film 358:16–21